



DOI: 10.22070/jqepo.2023.16031.1232

## Monitoring Serially Correlated Data by Two CUSUM Charts (Case Study: Numbers of Patients with Covid-19)

Ahmad Hakimi<sup>1</sup>, Hiwa Farughi<sup>1\*</sup>, Jamal Arkat<sup>1</sup>

<sup>1</sup> Department of Industrial Engineering, University of Kurdistan, Sanandaj, Iran

\* Corresponding Author: Hiwa Farughi (Email: [h.farughi@uok.ac.ir](mailto:h.farughi@uok.ac.ir))

---

**Abstract** –Statistical process control charts are utilized in many industries, including manufacturing, environmental monitoring and improvement, disease surveillance, and others. The use of statistical process control charts is common for independent process observations at different times. However, in the case of sequential data, correlation between the data is typically present. Therefore, the creation of control charts specifically for monitoring serially correlated data is essential. The Covid-19 epidemic is a severe global issue, with evidence indicating that infected individuals can transmit the virus to others, whose symptoms may appear several days later. This study aims to monitor the condition of Covid-19 patients over a specific period time using serial data. Two new CUSUM charts are used to track the number of Covid-19 patients in Iran, Japan, and Italy, with separate results presented and explained for each country. Additionally, a sensitivity analysis is conducted on key factors, yielding similar results, and the two control charts are compared.

**Keywords**– Covid-19, CUSUM chart, Data correlation, Patients number, Process monitoring.

---

### I. INTRODUCTION

Statistical process control charts, also called Shewhart charts or process-behavior charts, are utilized to assess if a business or manufacturing process is under control. These charts serve as a graphical device for Statistical Process Monitoring (SPM) and are crucial for management and control about quality in various industries, including disease monitoring. The cases of using control charts are extensive, for instance, monitoring car rear window in two stages profiles (Derakhshani, 2021) or in values education process (VEP) for students (Daneshmandi, 2020) that can be mentioned. Usual Statistical Process Control (SPC) charts, such as the Shewhart charts, cumulative sum (CUSUM) chart, exponentially weighted moving average (EWMA) chart, and change-point detection (CPD), are intended for situations in which process samples are independent at different time points (Montgomery, 2019, & Montgomery and Mastrangelo, 1991). However, in fact, process observations at different time points are almost always correlated with one another. The effectiveness of traditional SPC charts for independent observations has been shown to be questionable when dealing with serially correlated data, as discussed in Harris and Ross's 1991 study. Therefore, it is necessary to use new appropriate control charts that are monitoring serially correlated data. Serial correlation refers to

the connection among samples of the same variable in period time. If the serial correlation is zero, there is no connection between the observations, and each observation is independent. However, if the serial correlation deviation is towards one, the observations are serially correlated, and past values influence subsequent samples (Kim et al. 2007). In summary, a serially correlated variable follows a pattern and is not random. On the other hand, Serial correlation is used in statistics to describe the relationship between observations of the same variable over specific periods (Loredo et al. 2002). If a variable's serial correlation is measured as zero, there is no correlation, and each of the observations is independent of one another (Johnson and Bagshaw 1974). Conversely, if a variable's serial correlation skews toward one, the observations are serially correlated, and future observations are affected by past values. Essentially, a variable that is serially correlated has a pattern and is not random (Apley and Tsung 2002).

Several methods have been proposed for monitoring serially correlated data, such as parametric time series modeling and sequential residual monitoring. However, these methods have limitations, including sensitivity to assumed models and lack of robustness. Control charts for monitoring observations or residuals with assignable causes were introduced by Runger (2002), while robust exponentially weighted moving average (EWMA) charts were developed by Apley and Lee (2008). Adjustments to the control limits of conventional EWMA charts, aimed at accounting for uncertainty in estimated time series models, were later proposed by Lee and Apley (2011). While these modifications are a nice way to overcome limitations, they continue to depend on presumed parametric time series models that have predetermined orders and may not be trustworthy if the assumed models are incorrect.

To monitor serially correlated data, various methods have been proposed, including the CPD chart by Capizzi and Masarotto (2008) and Gaussian Process models by Alshraideh and Khatatbeh (2014). However, these methods have limitations, such as unjustifiable assumptions and the need for prior information about the correlation structure. Other researchers have suggested modifying traditional control charts or adjusting control limits, but some knowledge about the original data's correlation structure is still required. Recently, Qiu & Xie (2022) proposed transparent sequential learning for statistical process control, while Xue & Qiu (2021) proposed a nonparametric CUSUM chart. Zhou & Qiu (2022) suggested nonparametric profiles using mixed-effects modeling, and Li et al. (2019) proposed a CUSUM control chart wavelet-based nonparametric approach. These methods aim to overcome limitations and offer more reliable monitoring of serially correlated data.

A coronavirus-related respiratory disease recently occurred in the city of Wuhan in China. The World Health Organization named this coronavirus disease (COVID-19) after the first positive case of it in 2019 (WHO). The pandemic caused by COVID-19 has impacted almost every nation worldwide, resulting in the WHO categorizing it as a pandemic in March of 2020, according to sources such as Angulo et al. (2021) and Ayyoubzadeh et al. (2020). As well as, there are several articles in public health surveillance instance; Yuan et al. (2019) wrote a review paper about aberration detection algorithms used in monitoring public health. Furthermore, Aykroyd et al. (2019) proposed some recent developments in control charts, which have included non-Gaussian distributions and correlated data, with new applications in environmental science and tomography and considering modern statistical techniques such as wavelet methods.

In this article, two new CUSUM charts proposed by Qiu et al. (2020) and Li & Qiu (2020) are utilized. Two new flexible CUSUM charts were proposed, compared with five other charts, and their performance was discussed from various perspectives. Good performance was demonstrated by their methods, particularly in models with high autocorrelation in data. Consequently, in this paper, those charts are selected, and one of the essential variables of Covid-19, the number of patients, is examined. The rest of this paper is organized as follows. In Section 2, CUSUM charts for serially correlated data have been reviewed. Problem definition and research methods have been stated in Section 3. In Section 4, simulation study based on a real case along with interpretations for results have been presented and finally, concluding remarks and some suggestions for future research are stated in Section 5.

## II. CUSUM CHARTS FOR SERIALY CORRELATED DATA

CUSUM charts are widely used in quality control to monitor a process over time and are particularly effective in detecting small changes in the mean of a process. However, traditional CUSUM charts may not be effective when dealing with serially correlated data as they assume independence between observations. To address this issue, researchers have developed CUSUM charts for serially correlated data, which take into account the autocorrelation structure of the data. These charts can help identify small shifts in the mean of the process, even in the presence of autocorrelation, leading to improved quality control and process monitoring. Several studies have shown the effectiveness of CUSUM charts for serially correlated data in various fields, including healthcare and manufacturing.

The monitoring of serially correlated methods with an online type proposed by Qiu et al. (2020) and Li & Qiu (2020) represents the main methods used to process the data in this study. Observations must be serially de-correlated earlier than the online monitoring control chart in phase II, without the need for a time series model in parametric type and also about the parametric process distribution.

### A. New CUSUM Chart (N-CUSUM)

To evaluate the correlation structure of serial data and other in-control properties of the underlying process, it is necessary to have access to an in-control dataset. The estimated dataset, average and variance of the in-control (IC) can be denoted as  $\hat{\mu}_0$  and  $\hat{\sigma}^2$ , respectively. This assumption is made in our research paper.  $\gamma(q) = \text{Cov}(X_i, X_{i+q})$  only depends on  $q$  when  $i$  changes, and  $\gamma(q) = 0$  when  $q > T_{max}$ , where two process observations  $X_i$  and  $X_{i+q}$  are obtained at times  $i$  and  $i + q$  when the process is IC.  $T_{max}$  is chosen large and  $T_{max}$  can be chosen such that  $\gamma(q) \approx 0$  when  $q > T_{max}$ .

$$\hat{\gamma}_m(q) = \frac{1}{m-q} \sum_{i=-m+1}^{-q} (X_i - \hat{\mu}_0)(X_{i+q} - \hat{\mu}_0) \quad (1)$$

A two-sided CUSUM is employed here:

$$f_i = \max\{f_i^+, -f_i^-\} \quad (2)$$

Where,

$$\begin{aligned} f_i^+ &= \max[0, f_{i-1}^+ + (X_i - \hat{\mu}_0)/\hat{\sigma} - k] \\ f_i^- &= \min[0, f_{i-1}^- + (X_i - \hat{\mu}_0)/\hat{\sigma} + k], \text{ for } i \geq 1 \end{aligned} \quad (3)$$

$f_0^+ = f_0^- = 0$ , and  $k > 0$  is a fixed allowance. at time  $i$  the spring length is defined below:

$$T_i = \begin{cases} 0, & \text{if } f_i = 0 \\ b, & \text{if } f_i \neq 0, \dots, f_{i-b+1} \neq 0, f_{i-b} = 0 \end{cases} \quad (4)$$

See Qiu et al. (2020) for more information.

#### ❖ Calculation Parameters Monitoring Serially Correlated Data for CUSUM Chart:

1. In the case when  $i = 1$ , define the standardized observation at  $t_1$  to be  $e_1 = (X_1 - \hat{\mu}_0)/\sqrt{\hat{\gamma}_m(0)}$  Then, the charting statistic at  $t_1$  is defined to be:

$$f_i = \max\{f_i^+, -f_i^-\}$$

Where  $\tilde{f}_1^+ = \max\{0, e_1 - \tilde{k}\}$ ,  $\tilde{f}_1^- = \min\{0, e_1 + \tilde{k}\}$ , and  $\tilde{k} > 0$  is a fixed allowance. If  $\tilde{f}_1 = 0$ , then  $\tilde{T}_1 = 0$  and

otherwise, equal  $\tilde{T}_1 = 1$ .

2. In other case when  $i \geq 2$ , two states are proposed:

When  $\tilde{T}_{i-1} = 0$ ,  $\tilde{f}_i$  and  $\tilde{T}_i$  are calculated in the same manner as explained that in the case when  $i = 1$ .

However, if  $\tilde{T}_{i-1} > 0$ , define as below:

$$\hat{\Sigma}_{i,i} = \begin{pmatrix} \hat{\gamma}_m(0) & \cdots & \hat{\gamma}_m(\tilde{T}_{i-1}) \\ \vdots & \ddots & \vdots \\ \hat{\gamma}_m(\tilde{T}_{i-1}) & \cdots & \hat{\gamma}_m(0) \end{pmatrix} = \begin{pmatrix} \hat{\Sigma}_{i-1,i-1} & \hat{\sigma}_{i-1} \\ \hat{\sigma}_{i-1}^T & \hat{\gamma}_m(0) \end{pmatrix} \tag{5}$$

where  $\hat{\sigma}_{i-1} = (\hat{\gamma}_m(\tilde{T}_{i-1}), \dots, \hat{\gamma}_m(1))^T$ . For de-correlated the data use below equation:

$$e_i = \frac{X_i - \hat{\mu}_0 - \hat{\sigma}_{i-1}^T \hat{\Sigma}_{i-1,i-1}^{-1} e_{i-1}^*}{d_i} \tag{6}$$

Where  $d_i^2 = \hat{\gamma}_m(0) - \hat{\sigma}_{i-1}^T \hat{\Sigma}_{i-1,i-1}^{-1} \hat{\sigma}_{i-1}$ , and  $e_{i-1}^* = (X_{i-\tilde{T}_{i-1}} - \hat{\mu}_0, \dots, X_{i-1} - \hat{\mu}_0)$ . Li and Qiu (2016) found that  $e_i$  becomes uncorrelated with  $e_{i-1}, e_{i-2}, \dots$  as the sample size increases. This result was obtained through the Cholesky decomposition of the covariance matrix  $\hat{\Sigma}_{i,i}$ . The charting statistic is then defined as:

$$\tilde{f}_1 = \max\{\tilde{f}_1^+, -\tilde{f}_1^-\} \quad i \geq 2$$

Where

$$\tilde{f}_i^+ = \max\{0, \tilde{f}_{i-1}^+ + e_i - \tilde{k}\} \text{ and } \tilde{f}_i^- = \min\{0, \tilde{f}_{i-1}^- + e_i + \tilde{k}\}$$

If  $\tilde{f}_i = 0$ , then define  $\tilde{T}_i = 0$ . Otherwise, define  $\tilde{T}_i = \min(\tilde{T}_{i-1} + 1, T_{max})$ . A signal of mean shift for CUSUM chart defined in (3) and (4) gives when

$$\tilde{f}_i > \tilde{h}, \text{ for } i \geq 1$$

control limit define where  $\tilde{h} > 0$ .

**B. General CUSUM chart (G-CUSUM)**

This method proposed by Li & Qiu (2020) for monitoring serially correlated when observations are nonparametric and dependence. Also, this chart was named by them General CUSUM (G-CUSUM).

Let  $I_1 = (-\infty, q_1]$ ;  $I_2 = (q_1, q_2]$ ;  $\dots$ ;  $I_p = [q_p, +\infty)$  be a partition of the real line. Define  $Y_{nr} = I(X_n^* \in I_r)$  for  $r = 1, 2, \dots, p$ , and  $Y_n = (Y_{n1}, Y_{n2}, \dots, Y_{np})^T$ .

$Y_n$  is a vector with one element equal to 1 and the others equal to 0, representing the partitioning interval that  $X_n^*$  falls into. The IC distribution of  $Y_n$  is denoted as  $f^{(0)} = (f_1^{(0)}, f_2^{(0)}, \dots, f_p^{(0)})^T$ . If there is a shift in location or scale from the original observations' IC distribution, the distribution of  $Y_n$  will change from  $f(0)$ . Detecting this change allows for the identification of a location or scale shift in the original data's distribution. Then, the suggested nonparametric CUSUM chart is defined as follows:

$$C_n = (S_n^{obs} - S_n^{exp})^T \left( \text{diag}(S_n^{exp}) \right)^{-1} (S_n^{obs} - S_n^{exp}), \quad (7)$$

where,

$$\begin{aligned} S_n^{obs} &= S_n^{exp} = 0, && \text{if } D_n \leq k \\ S_n^{obs} &= (S_{n-1}^{obs} + Y_n) \frac{D_n - k}{D_n}, && \text{if } D_n > k \\ S_n^{exp} &= (S_{n-1}^{exp} + f^{(0)}) \frac{D_n - k}{D_n}, && \text{if } D_n > k \end{aligned} \quad (8)$$

and also  $D_n$  is equal to:

$$D_n = \{(S_{n-1}^{obs} - S_{n-1}^{exp}) + (Y_n - f^{(0)})\}^T \left( \text{diag}(S_{n-1}^{obs} + f^{(0)}) \right)^{-1} \{(S_{n-1}^{obs} - S_{n-1}^{exp}) + (Y_n - f^{(0)})\} \quad (9)$$

So,  $C_n > h$  is show the signal for this chart. For more information, see (Li & Qiu 2020).

### III. PROBLEM DEFINITION: NUMBER OF PATIENTS WITH COVID-19

The number of patients with COVID-19 in countries around the world has been a major topic of concern since the outbreak of the pandemic. The number of cases has varied greatly from country to country, with some nations experiencing a significant surge in infections while others have managed to keep the virus at bay. Factors such as the effectiveness of government response, availability of healthcare resources, and public compliance with safety measures have all played a role in determining the number of COVID-19 cases in each country. As the pandemic continues to evolve, monitoring and analyzing these numbers remains crucial for understanding the impact of the virus on global health and wellbeing. The SARS-CoV-2 virus is responsible for causing COVID-19, a respiratory illness that can range from mild to severe. While some individuals may not require specialized treatment, others may become critically ill and need medical attention. Individuals who are 65 years or older or have underlying medical conditions such as cardiovascular disease, diabetes, chronic respiratory disease, or cancer are at a higher risk of developing severe illness. COVID-19 can affect anyone regardless of age and can spread through respiratory droplets or aerosols when an infected person coughs, sneezes, speaks, sings, or breathes. These particles can vary in size from large respiratory droplets to tiny aerosols. (Middeldorp et al., 2020).

The previous section outlines a technique for monitoring a variable with autocorrelated data, which can be applied to many current issues. COVID-19 is a prominent issue facing the world today, and this method allows for a thorough examination of data and obtaining desired results through the use of charts. Real data on COVID-19 was obtained from [www.ourworldindata.org](http://www.ourworldindata.org), which included daily patient numbers, stringency index, vaccination rates, excess mortality, handwashing facilities, and other relevant information. This dataset covers the period from late 2019 when the disease first emerged.

The variable selected for analysis, as per the methodology outlined in section two, is the daily number of patients, measured in millionths. Previous studies (Middeldorp et al. 2020, Angulo et al. 2021, Ayyoubzadeh et al. 2020) have established that this figure is influenced by the number of patients seen in preceding days. Given that an infected individual can transmit the virus to multiple people, symptoms may manifest in subsequent days. The time between the virus entering a patient's body and the onset of symptoms (T max) is estimated by researchers to be approximately 8-20 days. In this study, T max is set at three different levels to explore their respective impacts. For another simulation, T max is set at 15 as this aligns with available data and is deemed appropriate and logical. The ensuing section will discuss the effects observed.

To select the variable for analysis, the ratio of patients per million was used, and a time interval for which country data was available was chosen. Data from January 3, 2020, to September 1, 2021, was selected, which was a couple of

months after the virus spread. Data from multiple countries, such as Iran, Japan, and Italy, was also examined to enhance the analysis. The trend of the proportion of patients per million is presented in the charts below.

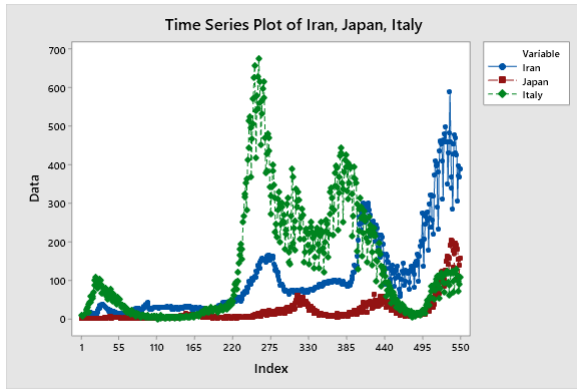


Fig. 1. Japan, Italy & Iran patients per million

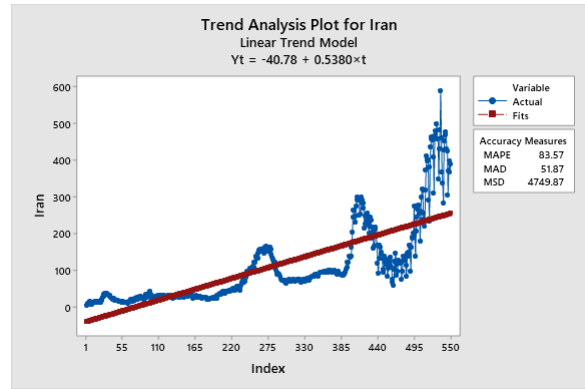


Fig. 2. Trend analysis for Iran's patients

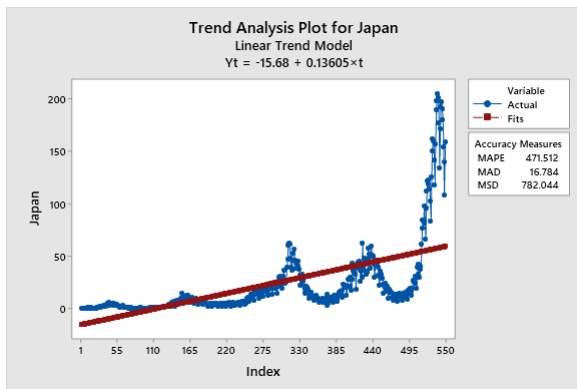


Fig. 3. Trend analysis for Japan's patients

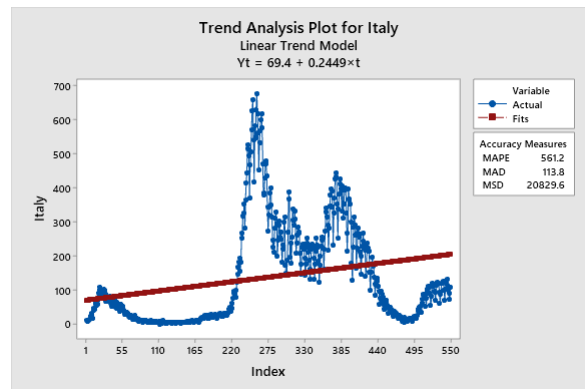


Fig. 4. Trend analysis for Italy's patients

The charts above illustrate the trend of the proportion of patients per million in various countries, including Iran, Japan, and Italy, from January 3, 2020, to September 1, 2021. The data was analyzed using trend lines and models generated through Minitab software. It is crucial to ensure equitable access to safe and effective vaccines to end the COVID-19 pandemic. Although many vaccines are being tested and developed, caution is still necessary since ongoing research examines how well vaccines protect against disease, infection, and transmission. Table I provides vaccination data for each country, including the start date of vaccination and the percentage of fully vaccinated individuals until September 1, 2021.

TABLE I. Date and total number of vaccination

	Iran	Japan	Italy
Vaccination start date	09 Feb 2021	17 Feb 2021	27 Dec 2020
Fully vaccinated per hundred (2021-09-01)	9.93	46.85	61.09

As a result, in Figs. 1-4, Iran begins vaccination with the 346th sample (day), Japan with the 354<sup>th</sup>, and Italy with the 302<sup>nd</sup>. However, as can be seen, the impact of vaccination on the incidence of new COVID-19 cases is not yet clear, except perhaps in Italy. Therefore, the data analyzed shows a similar pattern at present, and it is assumed that there is a correlation between the numbers of patients' data with a delay of around 15 days. This implies that the data being used to monitor the situation is not influenced by vaccination.

#### IV. A STUDY USING DATA TO SIMULATE AND ANALYZE THE IMPACT OF COVID-19 CASES

The focus of this section is to evaluate the effectiveness of the proposed control charts by using the OC ARL criterion with  $ARL_0$  set to 200. Additionally, a sensitivity analysis is conducted on the  $m$  and  $T_{max}$  sizes. The study utilizes a new statistic to monitor COVID-19 patients in three countries using 550 days of data from www.ourworldindata.org, resulting in 550 data points for each country. The results are generated through 5,000 simulation studies run by MATLAB software.

To demonstrate the impact of  $k$  at various shifts, it is assumed that a shift occurs at the beginning of Phase II process monitoring, with shift sizes ranging from 0 to 1. The control chart performance is compared under different shifts in  $k$  parameters in the table presented below.

TABLE II. Performance comparison of two control charts when  $ARL_0 = 200$

Control charts	$\delta$	0.1	0.25	0.5	0.75	0.9	1
	$\tilde{k}$						
N-CUSUM	0.1	116.78 (0.61)	91.23 (0.58)	69.35 (0.51)	35.49 (0.29)	22.09 (0.22)	14.28 (0.11)
	0.25	120.33 (0.70)	94.25 (0.53)	69.78 (0.49)	33.91 (0.31)	20.77 (0.22)	11.82 (0.09)
	0.5	121.97 (0.68)	94.18 (0.55)	68.77 (0.52)	32.66 (0.28)	19.79 (0.18)	10.02 (0.08)
G-CUSUM	$k=1$	121.67 (0.71)	98.55 (0.59)	72.41 (0.55)	36.75 (0.32)	24.01 (0.24)	15.97 (0.11)
	$k=2$	120.22 (0.92)	99.92 (0.60)	70.21 (0.51)	34.22 (0.39)	24.98 (0.28)	17.02 (0.13)

Calculated  $ARL_1$  values for Iran's in TABLE II, patients per million, data and  $T_{max} = 15$ . According to Table II, small  $\tilde{k}$  has better performance in small shifts and conversely. As can be seen,  $\tilde{k} = 0.25$  yields favorable results across all shift sizes, prompting its use in subsequent simulations. In addition, results show that, N-CUSUM has better performance than G-CUSUM based on  $ARL_1$  values.

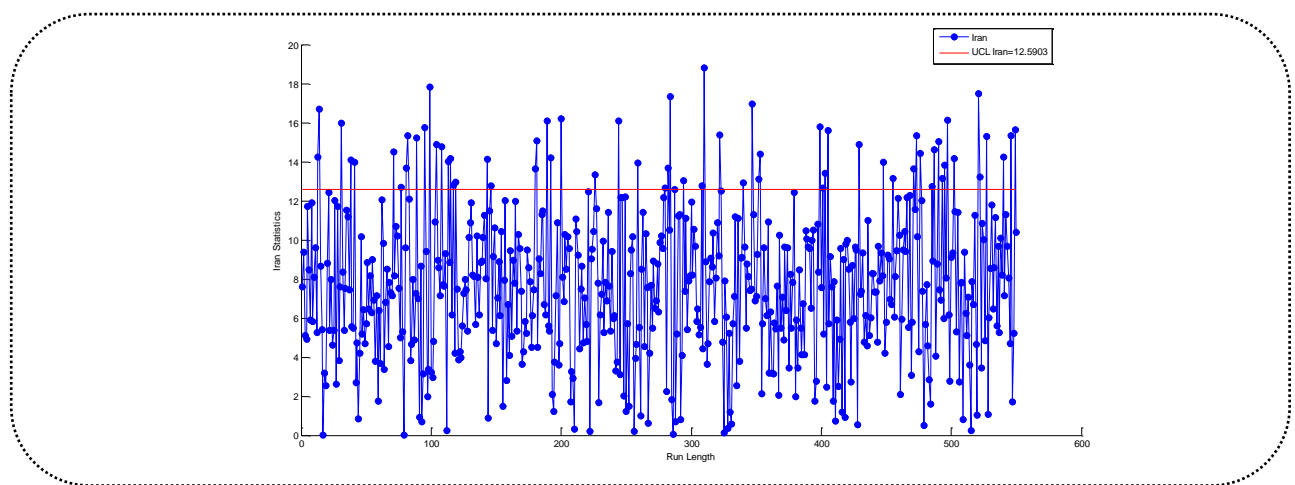


Fig. 5. Iran's number of patients run length and red horizontal line is UCL

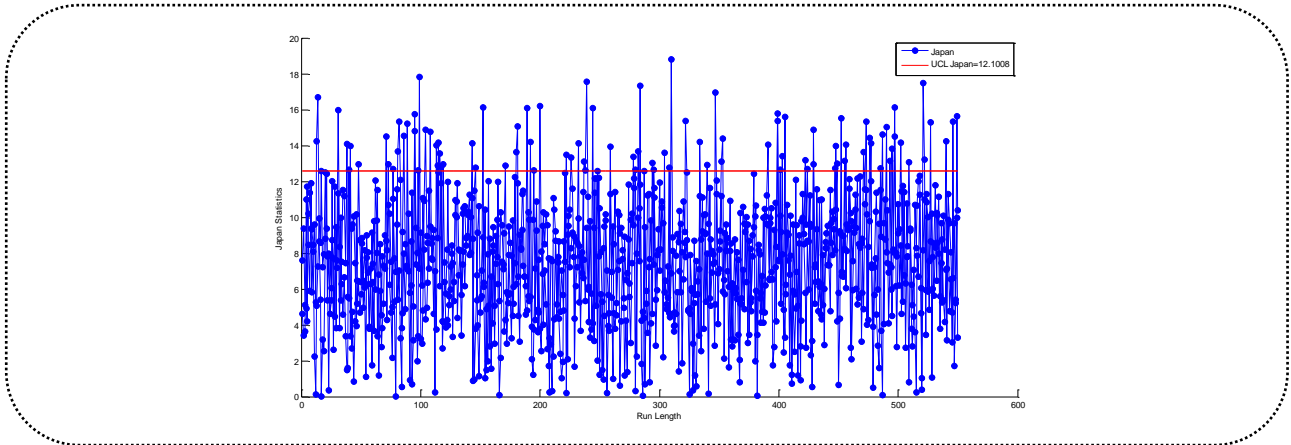


Fig. 6. Japan’s number of patients run length and red horizontal line is UCL

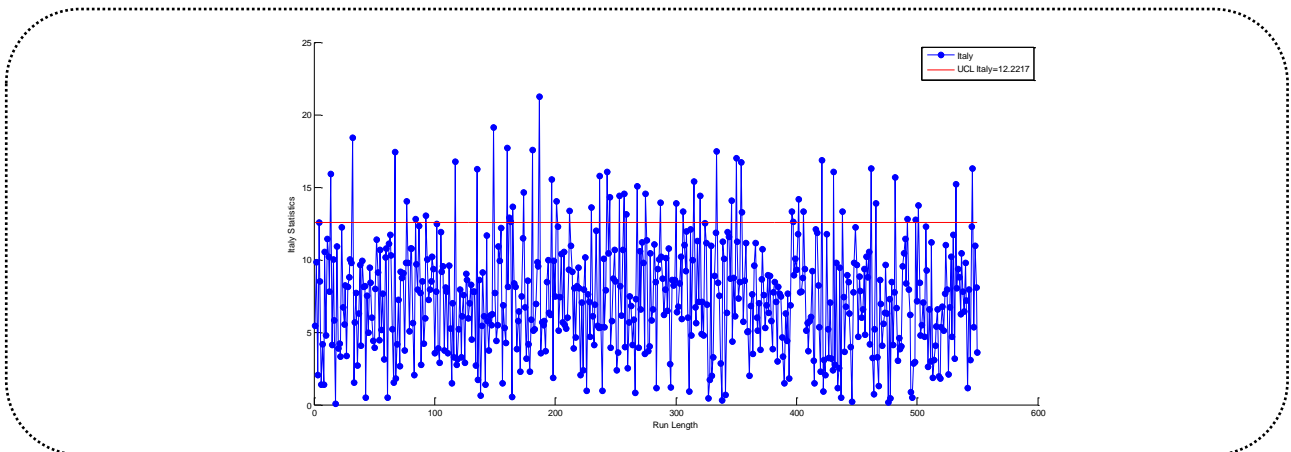


Fig. 7. Italy’s number of patients run length and red horizontal line is UCL

Using  $k = 0.25$ ,  $T_{max} = 15$ , and  $ARL_0 = 200$ , The charts in Figs. 5-7 indicate the duration of each country's outbreak. Iran's chart in Fig. 5 displays the initial signal at the 11<sup>th</sup> sample, while the charts for Japan and Italy in Figs. 6 and 7, respectively show the first signal at the 24<sup>th</sup> and 19<sup>th</sup> samples. As well as, in Figs. 5-7, the exact UCL values for each country can be seen on the right top.

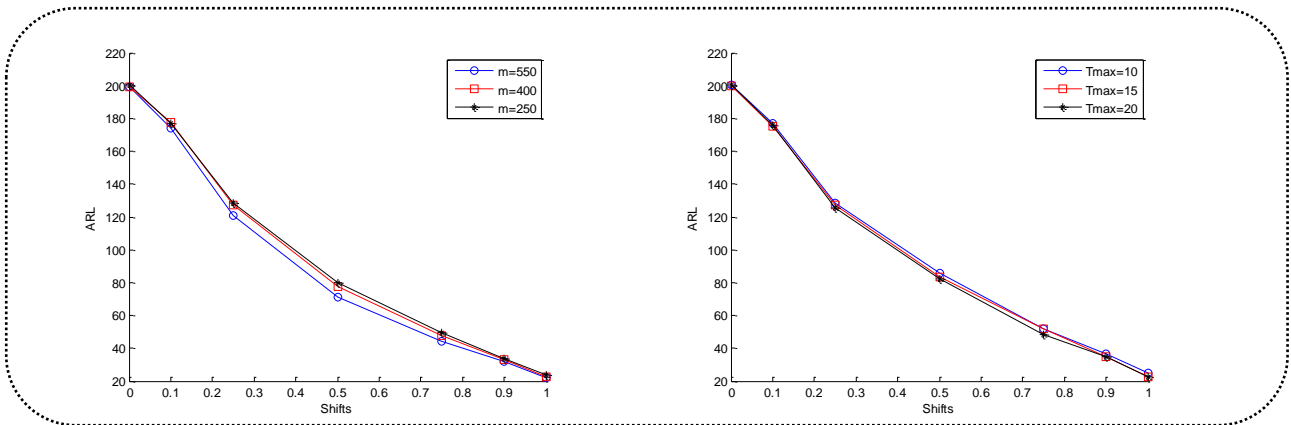


Fig. 8. The effect of  $m$  on  $ARL_1$

Fig. 9. The effect of  $T_{max}$  on  $ARL_1$

Furthermore, Figs. 8 and 9 demonstrate how the values of  $m$  and  $T_{max}$  impact  $ARL_1$  values for Iran's patient data. Fig. 8 reveals that larger values of  $m$  perform better and result in lower  $ARL_1$  values (specifically  $m=250$  and  $400$  at the end of the dataset). Fig. 9 shows the impact of  $T_{max}$ , indicating that there is little difference in small shifts between the three values (10, 15, and 20), but larger  $T_{max}$  values have better performance in larger shifts.

Additionally, a comparison of the two charts based on  $ARL_1$  is intended for this case. Accordingly, the table below presents these two charts under different shifts, with  $\tilde{k} = 0.25$  and  $k = 1$  or the N-CUSUM chart applied to Iran's patient data.

TABLE III.  $ARL_1$  values and their standard deviations (in parentheses) when  $ARL_0 = 200$

$\delta$ Chart	0.1	0.25	0.5	0.75	0.9	1	1.1
N-CUSUM	116.78 (0.61)	91.23 (0.58)	69.35 (0.51)	35.49 (0.29)	22.09 (0.22)	14.28 (0.11)	1.00 (0.02)
G-CUSUM	121.67 (0.71)	98.55 (0.59)	72.41 (0.55)	36.75 (0.32)	24.01 (0.24)	15.97 (0.11)	1.03 (0.03)

As mentioned in Table III, N-CUSUM control chart has better performance than G-CUSUM under all shifts in  $\delta$ . These results demonstrate that, N-CUSUM chart can detect the out-of-control condition faster than another charts for serially data based on the number of Covid-19 patients. In other words, this chart can warn of an increase or decrease in the number of Covid-19 patients in a shorter time.

**V. CONCLUSION AND FUTURE RESEARCH**

In this paper, the condition of COVID-19 patients was assessed and monitored using appropriate control charts. Two CUSUM-based control charts for serially correlated data were employed to track the number of COVID-19 patients in three countries: Iran, Japan, and Italy. Using two different control charts and three countries helps to analyze the data. The results for each country were displayed separately, and the effect of vaccination was observed. Similarly, when important factors are subjected to a sensitivity analysis, comparable outcomes are achieved, and the two control charts are compared. The result based on comparison  $ARL_1$  for two control charts showed that the N-CUSUM chart had better performance than G-CUSUM under all shifts in control schemes parameters. For future studies, developing these schemes for multivariate cases could be suggested and using these charts in similar issues that are affected serially are suggested.

**REFERENCES**

Alshraideh, H., and Khatatbeh, E. (2014). A Gaussian process control chart for monitoring autocorrelated process data. *Journal of Quality Technology*, 46(4), 317-322.

Angulo, F. J., Finelli, L., & Swerdlow, D. L. (2021). Estimation of US SARS-CoV-2 infections, symptomatic infections, hospitalizations, and deaths using seroprevalence surveys. *JAMA network open*, 4(1), 25-33.

Apley D.W., and Tsung, F. (2002). The autoregressive T 2 chart for monitoring univariate autocorrelated processes, *Journal of Quality Technology*, 34(1), 80-96.

Apley, D.W. and Lee, H.C., (2008). Robustness comparison of exponentially weighted moving-average charts on autocorrelated data and on residuals. *Journal of Quality technology*, 40(4), 428-447.

Aykroyd, R. G., Leiva, V., & Ruggeri, F. (2019). Recent developments of control charts, identification of big data sources and future trends of current research. *Technological Forecasting and Social Change*, 144, 221-232.

Ayyoubzadeh, S. M., Zahedi, H., Ahmadi, M., & Kalhori, S. R. N. (2020). Predicting COVID-19 incidence through analysis of google trends data in Iran: data mining and deep learning pilot study. *JMIR public health and surveillance*, 6(2), 50-56.

- Capizzi, G., and Masarotto, G. (2008). Practical design of generalized likelihood ratio control charts for autocorrelated data. *Technometrics*, 50(3), 357-370.
- Daneshmandi, A. A., Noorossana, R., & Farahbakhsh, K. (2020). Developing statistical process control to monitor the values education process. *Journal of Quality Engineering and Production Optimization*, 5(1), 33-54.
- Derakhshani, R., Esmaeeli, H., & Amiri, A. (2021). Monitoring binary response profiles in multistage processes. *Journal of Quality Engineering and Production Optimization*, 6(2), 97-114.
- Harris, T.J., and Ross, W.H. (1991). Statistical process control procedures for correlated observations, *The Canadian Journal of Chemical Engineering*, 69(1), 48-57.
- Johnson, R.A., and Bagshaw, M. (1974). The effect of serial correlation on the performance of CUSUM tests, *Technometrics*, 16(1), 103-112.
- Kim, S.H., Alexopoulos, C., Tsui, K.L., and Wilson, J.R. (2007). A distribution-free tabular CUSUM chart for autocorrelated data, *IIE Transactions*, 39(3), 317-330.
- Lee, H. C., & Apley, D. W. (2011). Improved design of robust exponentially weighted moving average control charts for autocorrelated processes. *Quality and Reliability Engineering International*, 27(3), 337-352.
- Li, J., Jeske, D. R., Zhou, Y., & Zhang, X. (2019). A wavelet-based nonparametric CUSUM control chart for autocorrelated processes with applications to network surveillance. *Quality and Reliability Engineering International*, 35(2), 644-658.
- Li, J., & Qiu, P. (2016). Nonparametric dynamic screening system for monitoring correlated longitudinal data. *IIE Transactions*, 48(8), 772-786.
- Li, W., & Qiu, P. (2020). A general charting scheme for monitoring serially correlated data with short-memory dependence and nonparametric distributions. *IIE Transactions*, 52(1), 61-74.
- Loredo, E., Jearekorn, D., and Borrer, C. (2002). Model-based control chart for autoregressive and correlated data, *Quality and Reliability Engineering International*, 18(6), 489-496.
- Middeldorp, S., Coppens, M., van Haaps, T. F., Foppen, M., Vlaar, A. P., Müller, M. C., ... & van Es, N. (2020). Incidence of venous thromboembolism in hospitalized patients with COVID-19. *Journal of Thrombosis and Haemostasis*, 18(8), 1995-2002.
- Montgomery, D.C. (2019), *Introduction to statistical quality control*. John Wiley & sons.
- Montgomery, D.C., and Mastrangelo, C.M. (1991). Some statistical process control methods for autocorrelated data. *Journal of Quality Technology*, 23(3), 179-193.
- Qiu, P., Li, W., & Li, J. (2020). A new process control chart for monitoring short-range serially correlated data. *Technometrics*, 62(1), 71-83.
- Qiu, P., & Xie, X. (2022). Transparent sequential learning for statistical process control of serially correlated data. *Technometrics*, 64(4), 487-501
- Runger, G.C., (2002). Assignable causes and autocorrelation: control charts for observations or residuals?. *Journal of Quality Technology*, 34(2), 165-170.
- Xue, L., & Qiu, P. (2021). A nonparametric CUSUM chart for monitoring multivariate serially correlated processes. *Journal of Quality Technology*, 53(4), 396-409.
- Yuan, M., Boston-Fisher, N., Luo, Y., Verma, A., & Buckeridge, D. L. (2019). A systematic review of aberration detection algorithms used in public health surveillance. *Journal of Biomedical Informatics*, 94, 103-116.
- Zhou, Q., & Qiu, P. (2022). Phase I monitoring of serially correlated nonparametric profiles by mixed-effects modeling. *Quality and Reliability Engineering International*, 38(1), 134-152.